Reports

Latitudinal and Longitudinal Oscillations of Cloud Features on Neptune

LAWRENCE A. SROMOVSKY

Voyager observations suggest that three of Neptune's major cloud features oscillate in latitude by 2° to 4° and that two of them simultaneously oscillate in longitude by 7.8° and 98° about their mean drift longitudes. The observations define most convincingly the two orthogonal oscillations of the second dark spot (near 53° south). These oscillations have similar periods near 800 hours and approximately satisfy a simple advective model in which a latitudinal oscillation produces a phase-shifted longitudinal oscillation proportional to the local wind shear. The latitudinal motion of the Great Dark Spot can be fit with an oscillation period of about 2550 hours, whereas its dominant longitudinal motion, if oscillatory at all, has such a long period that it is not well constrained by the Voyager data.

THE PERSISTENCE OF NEPTUNE'S MAJOR cloud features after their discovery during the long-range Voyager imaging observations (*1*) suggests that their lifetimes might significantly exceed the five months of Voyager observations. Some of these features may have been seen by ground-based observers as early as 10 years before Voyager (*2*) and probably will be seen again in images from the Hubble Space Telescope and ground-based observation. The unusual nonuniform motions of these cloud forms (*1, 3*) is of considerable concern in trying to link together these various observations to provide a window into the long-term atmospheric dynamics of Neptune. However, from position measurements and analyses reported here, it appears that simple empirical models incorporating sinusoidal oscillations can describe essentially all of the significant position variations of three of the major cloud features during the Voyager observation period.

The features of interest (Fig. 1) are the Great Dark Spot (GDS) at an average planetocentric latitude of 20.3°S (*4*), the bright Scooter (BS1) at 41.3°S, and the Second Dark Spot (DS2) at 53°S. We obtained relatively complete tracking coverage of these features from discovery to encounter by combining the Hammel *et al.* (*1*) position observations (their figure 2) with new independent observations (*5*). Relative to the start of Flight Data System (FDS) Counts (*6*), the Hammel *et al.* data extend from 7700 to 8820 hours, whereas our new data cover the periods from 7180 to 7490 hours and from 8550 hours to nearly the time of encounter at 9112 hours on 25 August 1989. Isolated preobservatory-phase Voyager observations at 5674 and 6890 hours were also included. This total range covers 213 rotations of Neptune (*7*).

The latitudinal accuracy of the observations was typically from 0.5° to 1°, varying with resolution and feature visibility. We corrected latitude measurements for errors in determining Neptune's orientation in the image frames by removing, for each feature, spurious correlations between latitude and distance to the central meridian. Longitudinal errors tended to be somewhat larger than 1° because of less sharply defined longitudinal boundaries of the features. Changes in shape of both the Scooter and the GDS contributed significant errors to some of the position determinations. The spectacular oscillation in the shape and orientation of the GDS (*7, 8*), which has a period of about 188 hours, appears unrelated to the oscillations in its central position.

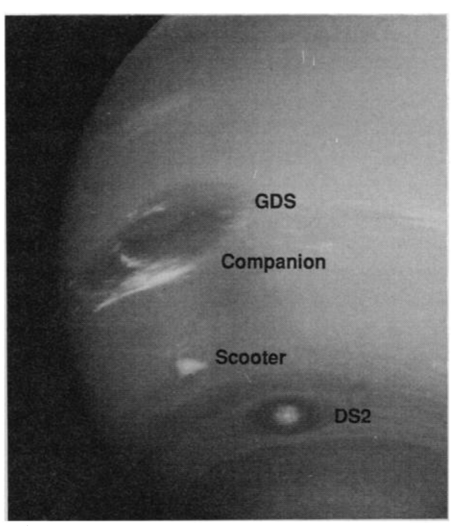

Fig. 1. Voyager 2 green-filtered image of Neptune's west limb, showing the GDS, the Companion cloud at the south edge of the GDS, the Scooter (the bright triangular feature), and the DS2 with a bright core. The Companion cloud remained in the same approximate location relative to the GDS during the entire span of Voyager observations.

The composite Voyager data set is shown in Fig. 2, A through C. The longitude data are plotted in rotating reference frames chosen individually for each feature to remove the large mean drift in longitude (hundreds to thousands of degrees during one oscillation). The Scooter and DS2 reference frames match the mean drift rates of the features determined by empirical fits described below. We chose the reference frame for the GDS to reveal details of the fit during the Voyager observation period (using the best-fit period would add a large ramp to both data and model, obscuring their differences).

The strongest evidence for a regular oscillation in latitude and longitude is seen in the DS2 data: considerably more than a complete oscillation is defined, and the oscillation amplitudes are large compared to measurement errors. There is also good evidence for a regular longitudinal oscillation of the Scooter, although its latitudinal oscillation is not as well defined because of its relatively small amplitude and because the observations do not quite span a complete cycle of motion. Only about 75% of a cycle of the GDS latitudinal oscillation is seen in the data with useful latitudinal accuracy. Although the GDS longitudinal data are compatible with an oscillation, they do not constrain very well the possible oscillation periods (as described below).

We initially modeled the motions of the features using a sinusoidal oscillation in latitude and an independent longitudinal oscillation about a mean drift rate:

$$\phi(t) = \phi_0 + C_\phi \sin[2\pi(t - t_0)/T_{\text{lat}} + \theta_\phi] \quad (1)$$

$$\lambda(t) = \lambda_0 + A\,(t - t_0) + C_\lambda \sin[2\pi\,(t - t_0)/T_{\text{lon}} + \theta_\lambda] \quad (2)$$

where $\phi(t)$ and $\lambda(t)$ are latitude and longitude at time t, T_{lat} and T_{lon} are oscillation periods, θ_ϕ and θ_λ are phases, C_ϕ and C_λ are oscillation amplitudes, and $A = u_0/R_{\text{rot}}$ is the mean longitudinal drift rate, where u_0 is the mean zonal speed and R_{rot} is the distance from the observed feature to the planet's rotation axis. These nonlinear models were fit by expanding the sine functions and using linear regression techniques. An approximation of χ^2 as a function of period was used to estimate the optimum period, and the uncertainty was estimated as the period change required to produce $\Delta\chi^2 = 1$ relative to the minimum.

Space Science and Engineering Center, University of Wisconsin-Madison, WI 53706.

The latitudinal fits (Table 1) are split into two sets. For the first set of fits (Fig. 2), T_{lat} was adjusted to minimize χ^2, with good results (the SD of the data from the fit is close to the estimated error in the observations). For the second set of fits (for the Scooter and DS2), T_{lat} was set equal to the optimum longitudinal period (from Table 2) to facilitate phase comparisons with the longitudinal oscillations. The GDS and DS2 latitudinal oscillation amplitudes are about twice that of the Scooter. The periods of the latitudinal oscillations vary almost linearly with the magnitude of $\sin(\lambda)$ but increase toward the equator (from 53°S to 20°S) by a factor of three.

Among the longitudinal fits (Table 2), the DS2 fit is the most convincing because it has the shortest period and completes almost two oscillations during the 1700-hour time span over which it has been seen in Voyager images. The DS2 is also interesting because $T_{lon} \approx T_{lat}$, suggesting a link between the two oscillations. For the Scooter, on the other hand, the best-fit T_{lon} is significantly longer than the best-fit T_{lat}, although neither are very tightly constrained by the data.

The most surprising result may be the longitudinal motion of the GDS, which, if oscillatory at all, appears to have an extremely long period; thus, it is not well constrained by the Voyager observations. For Voyager observations later than 7500 hours, the GDS longitudinal fit quality improves very slowly as T_{lon} is increased beyond several thousand hours. Including earlier observations at 5674 and 3981 hours leads to two types of good fits: one for $T_{lon} > 20{,}000$ hours and one for $T_{lon} \approx 8{,}000$ hours, with amplitudes of several thousand and several hundred degrees, respectively. To try to distinguish between them, we treated 1988 ground-based observations (*9*) of a bright cloud feature traversing Neptune's disk as if the feature were the Companion cloud (Fig. 1). This constraint still allowed two good fits: $T_{lon} = 26{,}500$ hours and $T_{lon} = 8{,}300$ hours, with standard errors of 2.48° and 2.24°, respectively. Earlier ground-based data (*10*) appear to favor the longer period fit, because this fit leads to larger period variations that are more compatible with the earlier observed periods. However, it is certainly not a clear choice because we cannot be sure that any of these ground-based observations are related to the GDS.

The residuals of the long-period GDS fits revealed a short-period component with approximately the same period as that of the GDS latitudinal oscillation. When a component of this type is added to the empirical model of the GDS motions, the fit quality improves significantly (SDs drop from 2.44° to 1.57°). This two-component fit is the one presented in Table 2 and Fig. 2. The shorter period component might be coupled to the latitudinal oscillation, whereas the longer period oscillation might arise from a different mechanism. A complete resolution of the GDS oscillation behavior will await further ground-based and space telescope observations.

We next consider an advection model that explains the longitudinal drift variations as a consequence of the latitudinal oscillations. This model assumes that the major cloud features move with the zonal component of atmospheric mass flow at their current latitudes (reaching equilibrium in a time short compared to the oscillation period T). For a local horizontal wind shear $du/d\phi$ and a latitudinal modulation given by Eq. 1, the advective model longitude equation becomes

Table 1. Fit parameters for latitudinal oscillation models. The bottom two rows are a second set of fits for Scooter and DS2 that use fixed periods equal to the longitudinal oscillation periods (Table 2) for better phase comparisons with the longitudinal oscillations. Because of poor latitudinal accuracy, data taken before the observatory phase (earlier than 7000 hours) were excluded from the GDS fit, and data taken before 7500 hours were omitted from the DS2 fits. Error limits are ±SE.

Feature	Mean latitude (ϕ_0)	Peak-to-peak oscillation amplitude ($2C_\phi$)	Period (T_{lat}, hours)	Phase (θ_ϕ)	SD from model (latitude)
		Fit period			
GDS	−20.34 ± 0.09°	4.20 ± 0.22°	2550 ± 100	−96.3 ± 3.5°	0.69°
Scooter	−41.30 ± 0.06°	2.08 ± 0.14°	1750 ± 90	−163.7 ± 6.0°	0.51°
DS2	−52.87 ± 0.06°	3.73 ± 0.18°	790 ± 10	−69.0 ± 2.4°	0.45°
		Fixed period			
Scooter	−41.26 ± 0.09°	2.10 ± 0.11°	Set to 1210	108.4 ± 6.6°	0.69°
DS2	−52.75 ± 0.08°	3.93 ± 0.22°	Set to 879.5	−37.0 ± 3.5°	0.61°

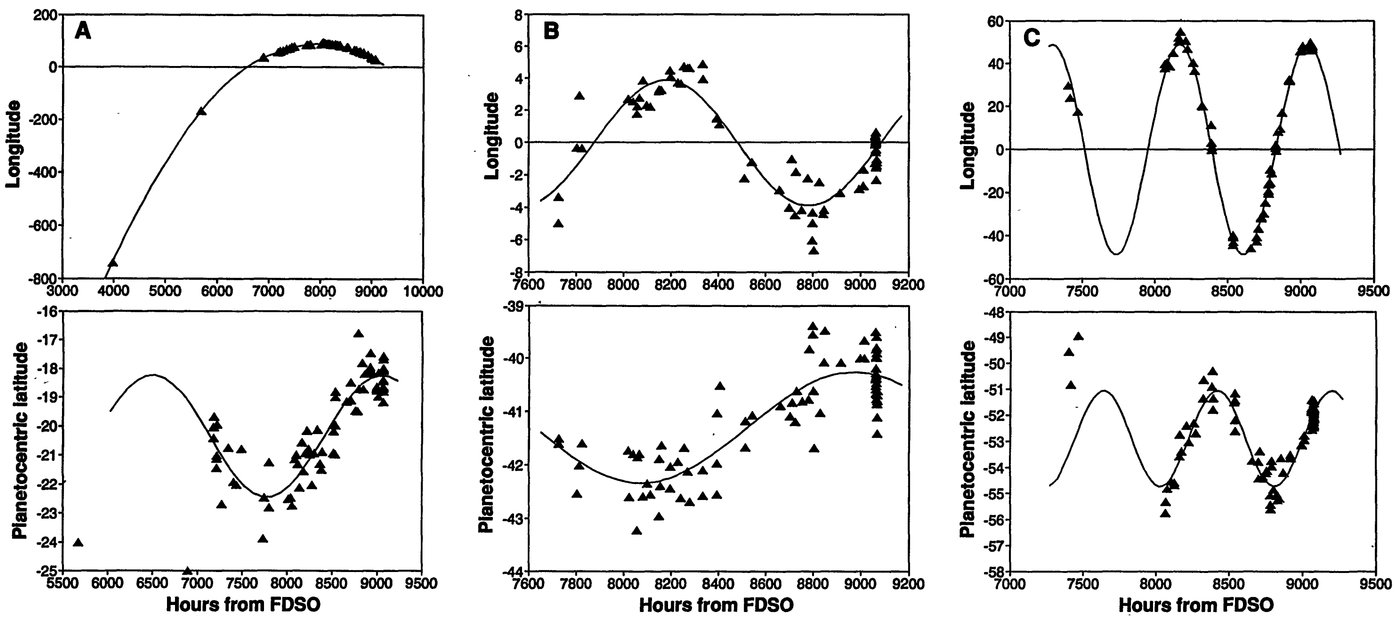

Fig. 2. Latitudinal and longitudinal oscillation model fits (solid curves) compared with observed positions (symbols) for (**A**) GDS, (**B**) Scooter, and (**C**) DS2. The longitudes are measured relative to rotating reference frames of periods 18.296 (A), 15.974 (B), and 16.752 hours (C).

Table 2. Fit parameters for empirical models of the longitudinal motions. A mean drift rate and a sinusoidal oscillation were determined by linear regression. The period of rotation about Neptune's spin axis was computed as $(A/360° + 1/16.11 \text{ hours})^{-1}$. Two superimposed oscillations were fit to the GDS observations (see text); although these oscillation periods are not true best-fit values, they do provide an excellent fit to the observations. Error limits are ±SE.

Feature	Rotation period (hours)	Peak-to-peak longitudinal oscillation amplitude ($2C_\lambda$)	Oscillation period (T_{lon}, hours)	Phase (θ_λ)	SD from model (longitude)
GDS	18.066 ± 0.012	3908 ± 32°	26,000	119.7 ± 1.5°	1.57°
		10.7 ± 0.5°	2,550	−32.4 ± 6.2°	
Scooter	16.7524 ± 0.0003	7.8 ± 0.4°	1,210 ± 100	−44.3 ± 3.2°	1.16°
DS2	15.9740 ± 0.0004	97.8 ± 0.9°	879.5 ± 2.0	48.3 ± 0.5°	2.28°

Table 3. Comparison of latitudinal and longitudinal oscillations. Only the DS2 and the short-period component of the GDS have phase shifts near that expected from the advection model (−90°) and, thus, warrant comparison of measured shears with those inferred from the advective model (column 4). Error limits are ±SE.

Feature	Phase shift ($\theta_\lambda - \theta_\phi - \pi$)	Longitude/latitude amplitude ratio (C_λ/C_ϕ)	Inferred $du/d\phi$ for 90° lag [m/(s − deg)]	Cloud top shear [m/(s − deg)]
GDS	−116 ± 7°	2.6	−1.4	−7.2
Scooter	27 ± 7°	6.4		−12.2
DS2	−94.2 ± 3.5°	26.8	−24	−13.2

$$\lambda(t) = \lambda(t_0) + (t - t_0)\, u_0/R_{rot} + (du/d\phi)\,[T/(2\pi R_{rot})] \times C_\phi \sin[2\pi(t - t_0)/T + \theta_\phi - \pi/2] \quad (3)$$

which implies, for $du/d\phi > 0$, that the longitudinal oscillation should have a phase lag of 90° relative to the latitudinal oscillation ($\theta_\lambda - \theta_\phi = -\pi/2$) and an amplitude proportional to the local wind shear (at the level that is controlling the feature motion), so that $(du/d\phi) = (C_\lambda/C_\phi)\, T/(2\pi R_{rot})$.

The test of this model is presented in Table 3, in which the second group of latitudinal fits from Table 1 (with $T_{lat} = T_{lon}$) is used to make a meaningful comparison of latitudinal and longitudinal phases. The longer period component of the GDS longitudinal fit is inconsistent with the advective model (and omitted from Table 3) because it would imply enormous latitudinal excursions that are not observed. The phase shifts for the Scooter are in such disagreement with the advective model that amplitude comparisons are meaningless. However, the advection model is qualitatively upheld for the DS2 motions and for the short-period component of the GDS motions. There is good agreement on phase lags, although there is not good quantitative agreement on amplitudes. Relative to a smooth shear profile obtained from a simple polynomial fit to the observed wind speeds as a function of latitude (*11*), the shears derived from the advective model amplitude ratio are twice as large for DS2 and one-fifth as large for the GDS. Because Voyager 2 infrared spectrometer observations of horizontal temperature gradients imply relatively small vertical wind shears (*12*), it seems unlikely that altitude differences will explain the large differences between the observed and inferred wind shears. More likely alternatives are that the true wind-shear profile has local variations that are obscured by the large variability in the observed winds or that the model is incomplete.

What is the origin of the oscillations? Are there features in the interior that act as perturbations every time the large-scale feature passes overhead? If this were the controlling factor, the important parameter would be the time taken for the feature to move 360° of longitude relative to the interior. For the GDS, Scooter, and DS2, these times would be 132, 419, and 1894 hours. But these periods do not match the observed ones. A possibility suggested for the oscillation of Jupiter's Great Red Spot (GRS) (*13*), that some other eddy at a nearby latitude interacts with the major feature every time it passes, might also be relevant here. Making the passage times equal the observed latitudinal oscillation periods requires latitude differences of ~0.35° for all features, differences that are much smaller than the features themselves and the latitudinal oscillation amplitudes of the features. The lack of an identified perturbation makes this possibility highly speculative. Could the oscillations involve perturbations by eddies that are at the same latitude but vertically displaced? If so, it seems strange that the period is a monotonically decreasing function of latitude, because the vertical shear is least near 53°S (*12*), where the oscillation period is shortest.

How do these oscillations compare with those of the GRS on Jupiter? The GRS oscillation (*14, 15*) has a comparable period (89.89 ± 0.11 days or 2160 ± 2.6 hours) but a much smaller longitudinal amplitude of ~1°. An accompanying latitudinal oscillation has not been seen, perhaps because it is too small (0.05° might be expected from the advective model). The GRS longitudinal oscillation has been observed often enough since 1968 to establish a somewhat variable oscillation amplitude. The origin of the oscillation remains unexplained. Another interesting characteristic of the GRS is that it has not maintained a uniform rotation rate about Jupiter's axis but has wandered in longitude by more than 1000° (*13*). The wandering and the variable amplitude of oscillation of the GRS suggest caution in making long-term predictions of the motions of Neptune's features and point out the need for continued observations.

REFERENCES AND NOTES

1. H. B. Hammel *et al.*, *Science* **245**, 1367 (1989).
2. B. A. Smith, H. J. Reitsema, S. M. Larson, *Bull. Am. Astron. Soc.* **11**, 570 (1979).
3. B. A. Smith *et al.*, *Science* **246**, 1422 (1989).
4. The planetocentric latitude of a point is the angle between the equatorial plane and the vector from the planet center to that point.
5. The Hammel *et al.* (*1*) longitude for the DS2 position at 8800 hours required a 25° shift to the east to match our new observations. No adjustment was required for the other features.
6. FDS count units are 0.8 hours; the offset is such that 1100-counts (8800 hours) occurs at 3.71 hours universal time (UT) on 12 August 1989 (*1*).
7. Using the interior rotational period of 16.11 hours of J. W. Warwick *et al.* [*Science* **246**, 1498 (1989)].
8. L. M. Polvani, J. Wisdom, E. DeJong, A. P. Ingersoll, *ibid.* **249**, 1393 (1990).
9. H. B. Hammel, *ibid.* **244**, 1165 (1989).
10. R. H. Brown, D. P. Cruikshank, A. T. Tokunaga, *Icarus* **47**, 159 (1981).
11. S. S. Limaye and L. A. Sromovsky, *J. Geophys. Res.*, in press.
12. B. Conrath *et al.*, *Science* **246**, 1454 (1989).
13. T. Gehrels, Ed., *Jupiter* (Univ. of Arizona Press, Tucson, 1976).
14. E. J. Reese, *Icarus* **17**, 57 (1972).
15. H. G. Solberg, *Planet. Space Sci.* **17**, 1573 (1969).

16. It is a pleasure to acknowledge the considerable help provided by S. Limaye and P. Fry in carrying out the Voyager image processing. This research was supported by a grant from the National Aeronautics and Space Administration (NASA) Neptune Data Analysis Program.

8 July 1991; accepted 4 September 1991